IOP Publishing Phys. Biol. 21 (2024) 016001 https://doi.org/10.1088/1478-3975/ad0a9a

Physical Biology

OPEN ACCESS

RECEIVED
22 June 2023

REVISED
28 October 2023

ACCEPTED FOR PUBLICATION
8 November 2023

PUBLISHED
17 November 2023

PAPER

Calcium regulates cortex contraction in *Physarum polycephalum*

Bjoern Kscheschinski[1], **Mirna Kramar**[1] and **Karen Alim**[1,2,*]

[1] Max Planck Institute for Dynamics and Self-Organization, 37077 Göttingen, Germany
[2] TUM School of Natural Sciences, Department of Bioscience, Center for Protein Assemblies (CPA), Technical University of Munich, Garching, 85748, Germany
[*] Author to whom any correspondence should be addressed.

E-mail: k.alim@tum.de

Keywords: acellular slime mold, mechano-chemical coupling, self-organization

Supplementary material for this article is available online

Abstract

The tubular network-forming slime mold *Physarum polycephalum* is able to maintain long-scale contraction patterns driven by an actomyosin cortex. The resulting shuttle streaming in the network is crucial for the organism to respond to external stimuli and reorganize its body mass giving rise to complex behaviors. However, the chemical basis of the self-organized flow pattern is not fully understood. Here, we present ratiometric measurements of free intracellular calcium in simple morphologies of *Physarum* networks. The spatiotemporal patterns of the free calcium concentration reveal a nearly anti-correlated relation to the tube radius, suggesting that calcium is indeed a key regulator of the actomyosin activity. We compare the experimentally observed phase relation between the radius and the calcium concentration to the predictions of a theoretical model including calcium as an inhibitor. Numerical simulations of the model suggest that calcium indeed inhibits the contractions in *Physarum*, although a quantitative difference to the experimentally measured phase relation remains. Unraveling the mechanism underlying the contraction patterns is a key step in gaining further insight into the principles of *Physarum*'s complex behavior.

The ability to generate flows is crucial for many aspects of life ranging from the transport of nutrients and signaling molecules to the spatial organization of an organism [1, 2]. For example, during embryonic development, the interplay of mechanical forces, flows and biochemical patterning actively deforms and eventually shapes the embryo [3, 4]. Force-generating proteins in conjunction with filamentous proteins form a meshwork that acts as an active material. The coordinated activity of these proteins regulated by signaling molecules results in forces that can deform the organism's shape and generate flows. Hence, mechanical pattern formation here is an interplay of the active material, the resulting flow as well as the advection–diffusion dynamics of signaling molecules.

The slime mold *Physarum polycephalum* is a suitable model organism to investigate the emergence of flow patterns [5]. The unicellular organism grows as a macroscopic network of tubes and is able to maintain long-scale contraction patterns that result in a shuttle streaming inside the tube transporting mass effectively within the network [5]. The contractions result in stress gradients along individual tubes, pushing the cytoplasm through the network, thus, enabling the organism to distribute nutrients and signals effectively [6]. *Physarum* is able to display complex behavior despite its relatively simple body plan and the lack of a central nervous system and the flow properties have been linked to its complex behavior [7–10]: As the peristaltic contractions are responsible for the transport within the organism they have been suggested to be crucial for the organism to respond to external stimuli and reorganize its body mass, coupling the behavior of *Physarum* to the stress gradients along the network [11]. Despite the central role of the peristaltic contractions in *Physarum*, the chemical basis for the emergence of coordinated contractions is not fully understood.

A potential signaling molecule is calcium, which is one of the most versatile signaling molecules [12]. It orchestrates manifold aspects of cellular life including fertilization, cell division, stress responses, and gene transcription [13–15]. However, its most prominent

role is its effect on actomyosin activity [16] making it a likely candidate for the key regulator for contractile stress in the slime mold *P. polycephalum*. The identity of the regulatory agent as well as the emergence of contraction patterns has been the focus of previous work: Purified actin and myosin from *Physarum* showed that actomyosin activity is suppressed in the presence of calcium [17, 18]. These observations suggest that in *Physarum* calcium binds myosin directly [19, 20], in stark contrast to muscles in animals where actomyosin is regulated via troponin. Yet, direct observations of the dynamics of calcium and contractions in *Physarum* are scarce. In droplet-shaped *Physarum* fragments calcium-specific fluorescent dyes were recorded in parallel to droplet size finding that the relaxation of contractility within a fragment is preceded by a calcium peak [21]. In tadpole-shaped *Physarum* fragments in parallel measurements of traction stress and the calcium concentration found both to oscillate in phase [22]. Both kinds of data do not allow direct assessment of the impact of flows transporting calcium, theoretically predicted to be the key for the emergence of long-range flows: In tube shape plasmodia consisting of an active viscoelastic phase enclosing a passive fluid, a chemical regulator activating the contractions stress of the cortex is predicted to create self-organized flow patterns [23]. Similarly, microplasmodia modeled as droplets, where the two phases are interpenetrated and calcium acts as an inhibitor, can exhibit mechanochemical waves [24, 25]. To compare theoretical models for the self-organization of actomyosin contractions by calcium via fluid flows arising from contractions and transporting calcium, observations of contractions and calcium in *Physarum* tubes are required.

In this study, we experimentally measure the ratiometric calcium concentration in *Physarum* employing a combination of fluorescent dyes, while simultaneously measuring the local tube diameter along the network. In this way, we determine the phase relation between the local calcium concentration and the tube contractions. The simple network geometry allows a direct comparison with theoretical predictions confirming the observed phase-shift to be in line with an inhibitory effect of calcium on cortex contractility, albeit quantitative differences in the phase-shift likely arise from experimental constraints.

1. Methods

1.1. Sample preparation

To obtain reproducible measurements, *P. polycephalum* networks are cultured from microplasmodia developed from sclerotia (Carolina Biological Supply). As *Physarum* fragments tend to fuse, the microplasmodia are constantly shaken in a liquid growth medium suppressing the fusion. The liquid medium was prepared following [26], where chicken embryo extract was replaced by hematin ($5\,\mathrm{g\,l^{-1}}$) [27]. For sample preparation, micro plasmodia are placed on a phytagel substrate ($12\,\mathrm{g\,l^{-1}}$, see supplementary materials). Phytagel substrates avoid the auto-fluorescence of agar and are more transparent than agar, which reduces the scattering of light and achieves a higher signal-to-noise ratio. To further improve the image quality, only a thin substrate layer of approximately 1.3 mm is used.

The samples are prepared by placing a drop of medium including a high density of microplasmodia on the substrate followed by a 10–20 min drying period. The plasmodia are fed with a single oat flake and the Petri dish is sealed. Networks grow to sizes of 1–2 cm suitable for microinjections within 1–2 days.

1.2. Fluorescent dyes and microscopy

To measure the concentration of free calcium concentration we inject the calcium indicator Calcium Green-1 (ThermoFisher), whose fluorescence intensity increases upon binding calcium by 14-fold. In order to reduce the aggregation of the dye in the sample, the dextran-bound form (10 000 MW) was used. As the height of the individual tubes varies during contractions, the calcium-sensitive dye is complemented by the unspecific, fluorescent dye Texas Red (ThermoFisher) with the same molecular weight. This combination of dyes was previously used in [22]. Both dyes are dissolved in distilled water in a concentration of $10\,\mathrm{mg\,ml^{-1}}$. The dyes are used in a ratio of 3 (Calcium Green-1) to 1 (Texas Red). Imaging the two dyes simultaneously accounts for the variation of the tube height as well as uneven illumination of the sample and spatially uneven concentration of the dye.

To image the calcium concentration, the two dyes are injected into the network using a microinjector (InjectMan 4, Eppendorf). Prior to the injection, the tip of the femto tip (Eppendorf) is broken to obtain a tip with a diameter of approximately $5\,\mu$m. Typical injection volumes are in the order of $0.1\,\mu$l. Injecting large volumes, i.e. above $1\,\mu$l, causes the injected tube to stall or even burst, preventing the dye from spreading within the network. At least two microinjections are performed close to the desired tube for imaging without being within the imaging region (figure 1(a)). As the injections induce local gelation of the cytosol, the number of injection spots is limited by the morphology of the network. A high number of junctions and branches close to the imaging spot allows for more injections. The injected sample is imaged rapidly to prevent the dye from aggregation limiting the imaging time. Nonetheless, the dyes are allowed to spread for 3–5 min. Afterwards, the network is cut to obtain single tubes and the remaining

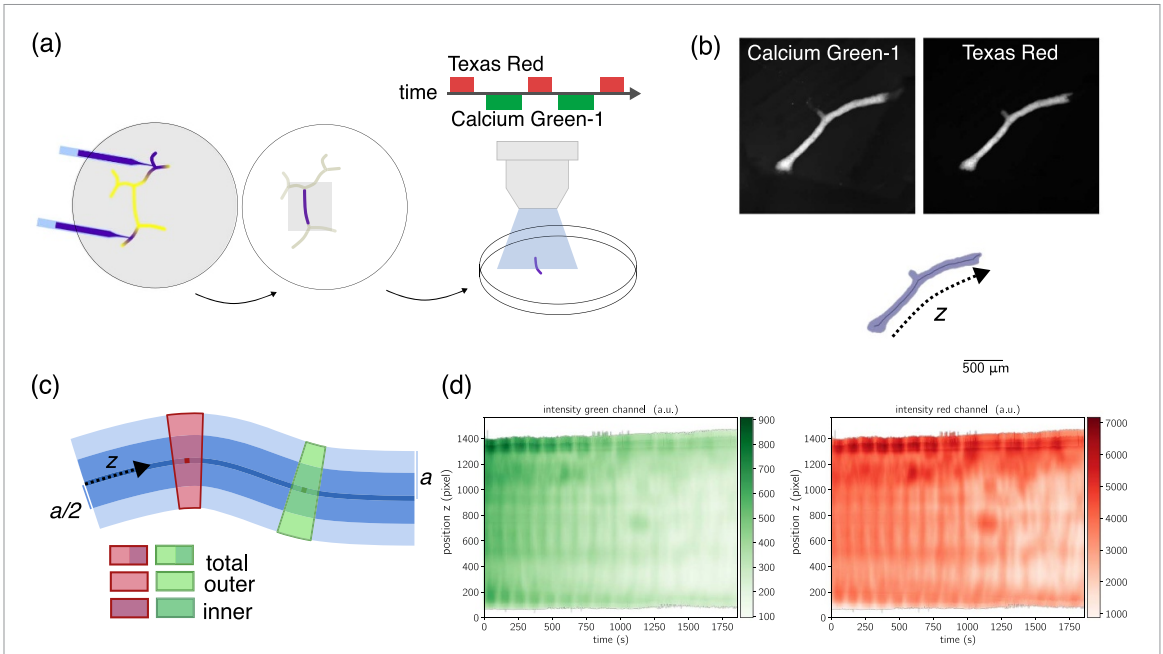

Figure 1. Experimental setup and image analysis. (a) Microinjections of Calcium Green-1 and Texas Red in the *Physarum* network surrounding the tube of interest followed by cutting the network isolating the chosen tube and imaging the sample. (b) For each frame, a mask and a skeleton are constructed. The skeleton defines the position z along the tube. (c) A slice of the tube is projected onto the skeleton of the network to obtain a one-dimensional representation of the sample. (d) Using the one-dimensional representation the intensity of the Calcium Green-1 and Texas Red dye are given as kymographs.

sample including the substrate is removed from the Petri dish with a spatula.

1.3. Imaging and image analysis

Around 5 min after the network is cut, the imaging is started. The samples are imaged using an Axio Zoom.V16 microscope (Zeiss) in two channels corresponding to the two fluorescent dyes, respectively. The dye Texas Red is imaged using the Zeiss filter cube 63 He and the dye Calcium Green-1 is imaged using the filter cube 46 He apart from the data set labeled C, where the filter cube 38 He was used. Excitation and emission wavelength are listed in the supplemental materials. The exposure time varies between the data sets depending on the strength of the fluorescent signal but is typically 1 s in the Calcium Green-1 channel and 0.5 s in the Texas Red channel. The resulting time resolution is about 3 s due to the limited speed at which the microscope can switch between channels.

To quantify contraction and ratiometric calcium dynamics image analysis is performed on the recordings as detailed below. In each frame, the network is separated from the background using a binary mask. The mask is calculated from the Texas Red channel using a threshold of 1.5 times the mean intensity of the entire frame. Secondly, based on the binary mask the center-line defined by the pixels equally distant to both edges is found. During the experiments, the network is cut into single tubes and thus the center-line skeleton is further reduced to a single branch (figure 1(b)). This one-dimensional representation is then used to project the intensity along the network by averaging over the orthogonal slice of the tube at every given position z along the skeleton of the tube (figure 1(c)). The local radius at time t of the tube along the skeleton $a(z,t)$ is determined as the minimal distance from the skeleton to the edge of the mask. The skeletonized networks of consecutive frames are aligned by finding the closest point in the skeleton to the previous reference point, where the first reference point is chosen to be the center point in the skeleton.

As the tube consists of two distinct phases, the wall and the enclosed cytoplasm, averaging over the entire tube slice removes differences caused by the two phases. Hence, pixels in the network are distinguished according to their distance to the skeleton relative to the local radius a. Positions in the network closer than $a/2$ are considered to be inner pixels, while larger distances correspond to outer pixels (figure 1(c)). This separation is not meant to reflect the actual wall thickness, as the wall thickness itself is inaccessible during the experiments. The inner and the outer parts of the tube will both include light emitted from the ecto- and the endoplasm. However, this separation is able to detect qualitative differences in the calcium dynamics, namely whether the calcium concentration in the endo- or ectoplasm precedes calcium concentration in the other phase. The average of the intensities is calculated separately over inner and outer pixels and the downstream analysis is applied to the cross-sectionally averaged signal as well as to the inner and outer signals.

In summary, we obtain the radius $a(z,t)$ and an averaged intensity along the network for each

frame $I(z,t)$ for both channels, namely the Calcium Green-1 and the Texas Red channel (figure 1(d)). Furthermore, we obtain an intensity only for the central, inner part of the tube $I_{\text{inner}}(z,t)$ and an intensity for the outer part of the tube $I_{\text{outer}}(z,t)$.

1.4. Numerical integration and model parameters

The theoretical model (section 2) is solved numerically using a θ-weighted Crank–Nicholson scheme ($\theta = 0.55$). The rest radius and the length of the tube are set to $a^* = 100\,\mu$m and $L = 10$ mm, respectively. The diffusion coefficient of calcium in the cytoplasm is assumed to be $D = 2 \times 10^{-10}\,\text{m}^2\,\text{s}^{-1}$ [24, 28]. The rheological parameters of the cortex and the fluid are only approximately known and might vary depending on the state of the organism [29]. The viscosity of the cortex is estimated with $\eta = 200$ Pas, while the elasticity is either set to $E = 2$ Pa or $E = 20$ Pa. The viscosity of the cytoplasm is set to $\mu = 1.5 \times 10^{-3}$ Pas. The strength of the non-linearity of the cortex stress $\kappa = 1000$ Pa is set to obtain typical contraction amplitudes. The deformation length scales are set to $\varepsilon_c = 0.3$ and $\varepsilon_\sigma = 2$. Finally, d_c and p_c determining inflow and capturing rates of calcium need to be set. The parameter p_c determines the steady-state concentration of calcium. Since the concentration can be freely re-scaled we choose $p_c = 1$. Then, the parameter d_c is absorbed in a time scale $\tau = 2d_c/a^*$ determining how quickly the concentration is regulated for a given cortex stretch. The time scale is set to 32 s and 100 s and the parameters of the active stress are set to $\sigma_0 = s = 36$ Pa and $\sigma_0 = s = 100$ Pa for the simulation with $E = 2$ Pa and $E = 20$ Pa, respectively. These parameter choices result in similar radius amplitudes and contraction frequencies in the two simulations. The simulations are conducted with closed boundary conditions. Hence, the mass transport of calcium as well as the flow velocity vanish at the tube ends. The initial conditions are set by perturbing the steady state of the radius a and the integrated concentration $\mathcal{C}$ with uncorrelated, Gaussian noise with a standard deviation of 1% around the respective steady-state value.

2. Results

2.1. Calcium concentration and tube radius are close to anti-phasic

Parallel measurements of the fluorescent signal of the calcium-sensitive dye Calcium Green-1 and the unspecific dye Texas Red together with the tube radius dynamics allow us to relate the contraction dynamics of the tube to the calcium concentration. Fluorescence in the green and red channels as well as the tube radius are measured along the one-dimensional representation, the skeleton, of the excised tube every 3 s. As the network evolves over time, we restrict the analysis to positions along the skeleton that are part of the skeleton for the entire experiment. Furthermore, we account for the time delay between the imaging in the two channels due to the switching of the respective filter cubes. Thus, the time series are interpolated and shifted with respect to each other by half a frame resulting in a symmetric relation of the signals avoiding inherent shifts. Finally, the ratio between the average intensities of the green and the red channel yields the cross-sectionally averaged concentration,

$$C(z,t) \propto \frac{I^{\text{Calcium Green}}(z,t)}{I^{\text{Texas Red}}(z,t)}. \tag{1}$$

Even though the concentration is only known up to a constant prefactor, this ratio independent of variations in tube volume due to contractions is referred to as calcium concentration. Kymographs for four data sets of the tube radius and the calcium concentration are shown in figures S1–S4. To investigate the interplay of calcium and contractions, we calculate the phase-dependent calcium concentration. For that each time point is assigned to a contraction phase ϕ using a Hilbert transform (see (d) in S1–S4). The phase is calculated based on the band-passed radius time series with a band-pass set to be ± 5 mHZ around the dominant frequency, which typically is around 10 mHZ. A phase-dependent calcium signal $C(\phi)$ is calculated by averaging over the calcium concentrations in the kymograph $C(z,t)$ assigned to the same binned instantaneous phases.

Finally, the shift is determined as the phase shift between the main oscillation of the radius and the concentration approximated by a sinusoid, such that a shift of 0 indicates an anti-phasic relation and a positive shift indicates that the radius peaks before the calcium concentration reaches its minimum. Photobleaching of the fluorescent dyes is slow compared to the contraction time scale of the tubes and equally affects the measured calcium concentration at different phases. Thus, the phase shift calculated here is robust against this experimental limitation.

We find that the calcium concentration approximately peaks when the radius is minimal and vice versa (figure 2(a)). The determined deviation from an anti-phasic relation is smaller than $\phi/4$ (figure 2(a)) and all four data sets show positive phase shifts (figure 2). Furthermore, the phase averaged signals (figure 2) reveal that the signal corresponding to the inner calcium concentration reaches its minimum earlier than the outer concentration.

To assess the contribution of potential auto-fluorescence or uneven Calcium Green-1 concentration in the tube cross-section, we consider the following case: Assuming the entire auto-fluorescent material is located in the tube walls and only contributes to the signal measured in the Calcium Green-1 channel, the ratiometric signal is shifted towards an anti-correlated relationship between the radius and calcium concentration (see also supplementary 3 and figure S5). Similarly, an accumulation

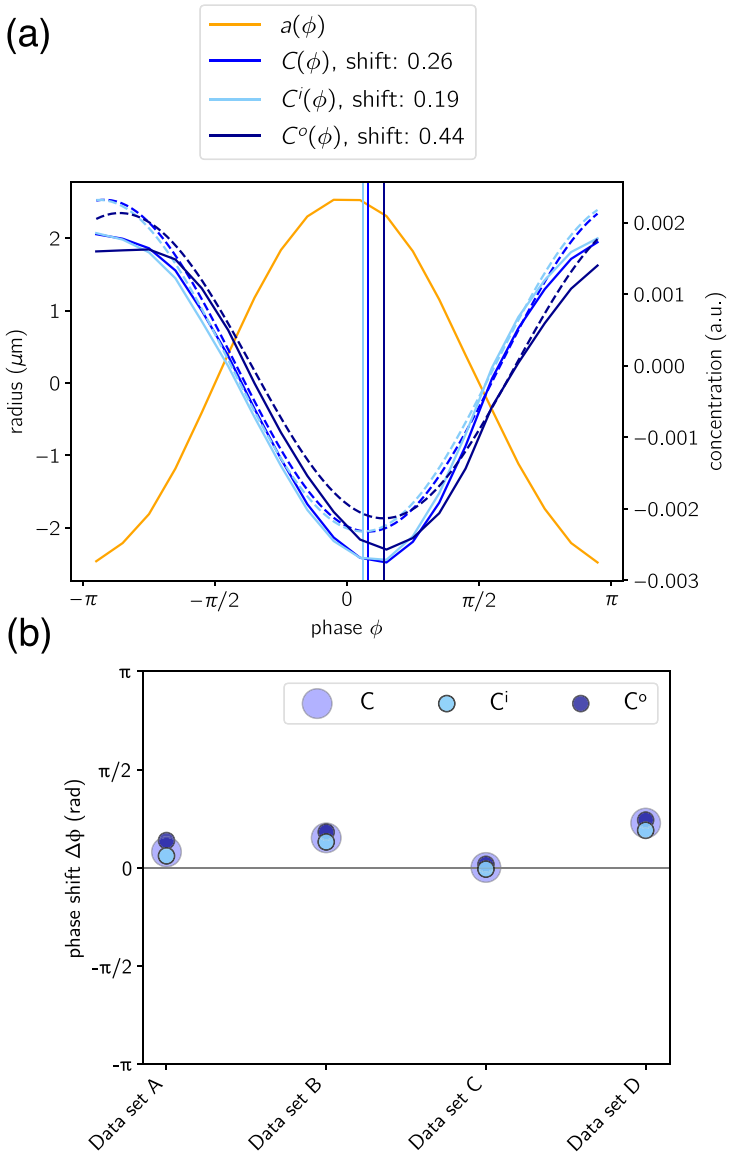

Figure 2. Anti-correlated relation between radius and calcium signal. (a) The total concentration $C(\phi)$, inner concentration $C^i(\phi)$, and outer concentration $C^o(\phi)$ as a function of the phase of the contraction of the tube shows a relation which is close to anti-phasic, but with a clear positive shift meaning that the radius peak precedes the minimum in the calcium signal. (b) Phase relation of radius and calcium signal consistently indicates a nearly anti-phasic, positive shift. Data set A is the data set shown in (a).

of Calcium Green-1 bound to calcium in the tube cortex would shift the ratiometric signal in the same way. Thus, we regard the measured phase shift as a lower bound, and the true phase shift might be larger.

2.2. Phase relation of the theoretical model is shifted by the cortex properties

As calcium concentration interacts with the cortex, which is itself driving contractions that generate fluid flows that are shuttling calcium around, theoretical models help disentangle how calcium affects the cortex.

To investigate the phase relation for calcium acting as an inhibitor, we formulate a theoretical model. Note, that we here aim for the minimal amount of the assumptions to gain mechanistic insight on the qualitative predictions of the model rather than over-modelling for the pursuit of quantitative agreement with data. Thus, the model couples the contractile stress to the concentration of calcium, while the inflow of calcium depends on the stretch of the cortex following [23]. The model describes a tube consisting of a fluid phase and an enclosing visco-elastic cortex, where the active stress of the cortex is inhibited by the calcium concentration. At the same time, the calcium concentration is coupled to the stretch of the cortex.

The tube is radially symmetric, and, thus, the tube shape is fully described by the radius $a(z,t)$ that depends on the position along the tube z and time t.

The continuity equation in terms of the tube radius reads,

$$\frac{\partial a^2}{\partial t} = -\frac{\partial}{\partial z}\left(a^2 U\right). \tag{2}$$

Radial deformations of the tube are written as $\varepsilon = (a - a^*)/a^*$, where a^* is the rest radius.

The cortex stress σ_c is the cause of the pressure gradient along the tube and, thus, the cross-sectionally averaged flow velocity U reads,

$$U = -\frac{a^2}{8\mu}\frac{\partial \sigma_c}{\partial z}.$$

The key assumptions of the model are the coupling of the cortex stress σ_c to the calcium concentration as well as the coupling of the capturing rate of calcium to the deformations of the tube ε. Specifically, in the model, calcium inhibits the contraction of the tube and flows in as the tube is contracted. The cortex stress is modeled by a passive visco-elastic part described by a Kelvin–Voigt model with an additional non-linear term and an active part that depends on the calcium concentration.

$$\sigma_c = E\varepsilon + \kappa\varepsilon^3 + \eta\frac{\partial \varepsilon}{\partial t} + \left[\sigma_0 - s\frac{\mathcal{C}}{\mathcal{C}+\mathcal{C}^*}\right]\left(1 - \frac{\varepsilon}{\varepsilon_\sigma}\right), \tag{3}$$

where E is the elasticity, κ the strength of the non-linearity, and η the viscosity of the cortex. $\mathcal{C}$ is the cross-sectionally integrated calcium concentration with $\mathcal{C}^*$ being its equilibrium value. For the active stress term, s is related to the slope of the tension at physiological concentrations and may be interpreted as the sensitivity to concentration changes. The parameter σ_0 determines the amplitude of the tension.

The calcium dynamics reads,

$$\frac{\partial \mathcal{C}}{\partial t} = \frac{\partial}{\partial z}\left[-U\mathcal{C} + \left(D + \frac{U^2 a^2}{48D}\right)a^2\frac{\partial}{\partial z}\left(\frac{\mathcal{C}}{a^2}\right)\right] + 2\pi a\left[p_c - d_c\left(1 + \frac{\varepsilon}{\varepsilon_c}\right)\frac{\mathcal{C}}{\pi a^2}\right]. \tag{4}$$

The first term describes the transport of calcium along the tube governed by Taylor-dispersion [30, 31]. As calcium triggers the contractions of the tube, the inflow of calcium is dependent on the stretch of the cortex creating a feedback loop. Deformation-induced regulation in eukaryotic cells has been found experimentally [32–34]. Especially the knowledge about mechanosensitive calcium channels [35] motivates the source term. The relevant length scale of the deformation for the deformation-dependent calcium capturing is represented by ε_c. The parameters p_c and d_c determine the strength of the inflow and capturing, respectively. Notably, the cross-sectionally averaged calcium concentration and the radius of the tube are the properties we determine from the experimental data.

The rheological properties of the cortex determine how the cortex responds to stress. Thus, the elasticity and the viscosity in the Kelvin–Voigt model affect the relation of the tube radius to the calcium concentration. We consider two contrasting cases: A cortex with a high viscosity η yielding $\gamma = \frac{\eta f}{E} \sim 10^{-1}$ and low elasticity and a cortex with high viscosity and high elasticity E such that $\gamma \sim 1$. To achieve that, the elasticity is set to $E = 2\,\mathrm{Pa}$ and to $E = 20\,\mathrm{Pa}$, respectively, while the viscosity is unchanged.

The altered rheological properties of the tube cortex affect the phase shift between the full relaxation of the tube and the peak of the calcium concentration: For a cortex with a high elasticity (figure 3(b)), the phase shift is larger than for a cortex with a high viscosity (figure 3(d)). Thus, as the viscous term becomes more important relative to the elastic term in the Kelvin–Voigt model, the radius signal is delayed relative to the active tension. At low elasticity, the phase relation approaches the experimentally observed phase shift, but there remains a quantitative difference to the relation found experimentally which is closer to anti-phasic than the predicted one.

3. Discussion

We investigated the role of calcium in the self-sustained contraction patterns of the cortex of *Physarum*. Ratiometric measurements provide an experimental way to account for a varying tube thickness when measuring the intracellular free calcium concentration in *Physarum*. It allows us to measure the instantaneous phase of calcium oscillations, which can be related to the contractions of the tube. Imaging the calcium dynamics involves exposing the *Physarum* networks to microscope light that can act as stimulus [36] impacting intracellular mechanisms. Importantly the networks are entirely illuminated, and the microscope light does not induce directed motion of the network. The experimentally observed relation between calcium and radius is nearly anti-phasic in line with previous findings with calcium indicators [21, 37]. Notably, all of the samples exhibit a positive phase shift. This finding indicates that the peak of the radius precedes the minimum of the calcium concentration, pointing to a contraction-inhibiting role of calcium.

The simple geometry of the experimental samples allows direct comparisons with a previously introduced theoretical model [23], which is adapted here to feature an inhibiting effect of calcium on the actin-myosin activity. Calcium locally inhibits the contractility of the cortex, while the stretch of the cortex regulates the inflow of calcium into the endoplasm. Since the contractions of the cortex induce endoplasmic flows, calcium is transported along the tube, which results in self-organized flow patterns. We find

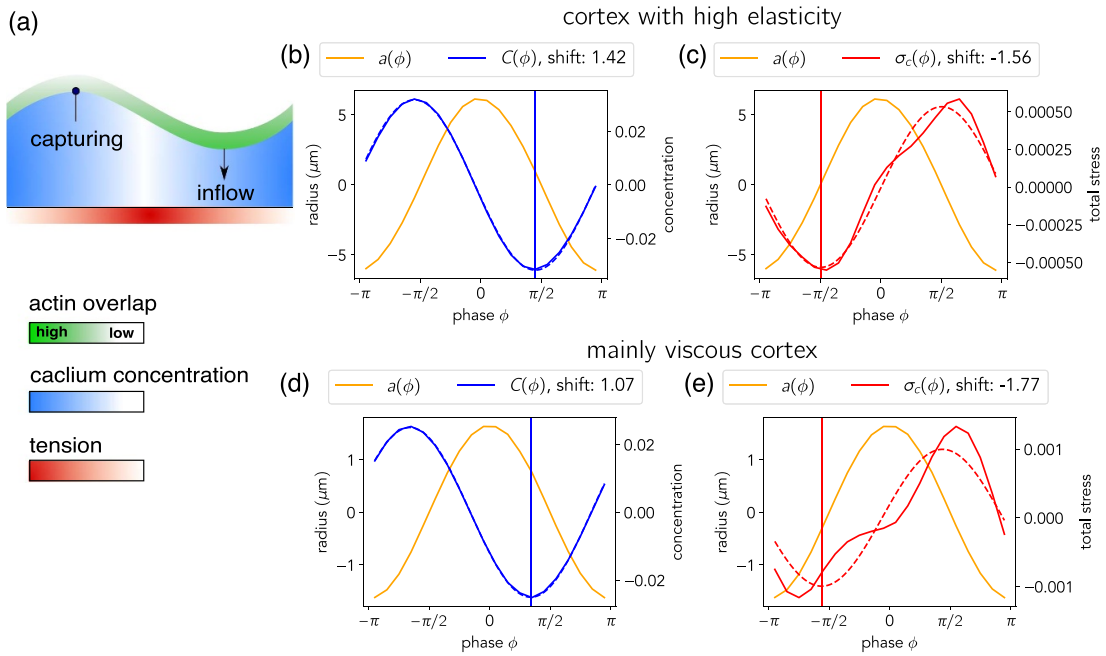

Figure 3. Theoretical model with an inhibiting calcium effect predicts a phase shift depending on the cortex properties, but smaller than $\pi/2$. (a) In this model, calcium inhibits the active stress of the tube cortex leading to the deformation of the tube ε. Depending on the tube radius the overlap of actin in the cortex increases cortex stress when the tube radius is small leading to strong tube deformation which eventually triggers the inflow of calcium. (b) For a cortex with high elasticity the phase relation between the calcium and the radius is close to $\pi/2$. (c) The cortex stress shows a shift of almost $\pi/2$. (d) For a mainly viscous cortex the phase relation is shifted left towards the anti-correlated relation that is observed in the experimental data. (e) The cortex stress oscillation is shifted in the same direction relative to the cortex stress oscillation shown in (c).

the precise phase relation between the calcium concentration and the tube radius depends on the rheological properties of the cortex: The phase shift predicted by the model is close to $\pi/2$ when the cortex mainly acts elastically. For a predominantly viscous cortex with a lower elasticity, the phase shift decreases and approaches the experimentally observed phase shifts. For physiological parameters, a quantitative difference between the theoretically predicted and the experimentally observed phase relation remains.

Since it is experimentally not possible to exclude the contribution of the cortex to the overall calcium signal, the measured calcium concentration is a mixture of the fluorescence of the ectoplasm and the endoplasm of the tube. Potential effects due to the accumulation of Calcium Green-1 bound to calcium in the cortex and due to auto-fluorescence of the tube cortex could affect the quantification. As shown in the supplementary materials, an enrichment of fluorescence in the cortex may shift the measured phase relation between the radius of the tube and calcium concentration towards an anti-phasic relation. Due to the geometry of the tube, the calcium signal close to the center of the tube is less affected by the cortex accumulation. Notably, we find that the inner calcium signal consistently precedes the outer calcium signal in the four data sets. This suggests that the phase shift of the endoplasm is indeed greater than the experimentally measured one. Our observations, therefore, indicate that the true phase shift of the endoplasmic calcium concentration is between the detected phase shift, which serves as a lower bound, and $\pi/2$. Given that a living *Physarum* plasmodium is very dynamic with high responsiveness to external stimuli, the consistent differences in the phase dependence of the calcium concentration close to the center of the tube and farther outside the center hints at a robust underlying mechanism.

While our model does not take into account the spatial differences across the tube cross-section and potential time delays between the tension of the cortex and the cross-sectionally averaged calcium concentration, it successfully captures the core relationship between calcium and contraction dynamics, i.e. the inhibiting effect of calcium on the actin-myosin activity in *Physarum*. This finding is in line with previous work [17, 18, 21, 24] and expands on it by providing real-time measurements of calcium dynamics in a long tube of live, contracting plasmodium.

Understanding the interplay of actomyosin activity, cytoplasmic flows, and calcium concentration in *Physarum* networks is essential as the resulting contraction patterns are at the basis of many intriguing behaviors of the slime mold. The success of the synergy of experiments and modeling in the single *Physarum* tube—the building block of a plasmodial network—presented here encourages, as well

as provides the groundwork for further studies on mechanochemical coupling in a living plasmodium over the multitude of its fascinating behaviors.

Data availability statement

All data that support the findings of this study are included within the article (and any supplementary files).

Acknowledgments

We would like to thank Markus Bär and Carsten Beta for several interesting discussions. This work was supported by the Max–Planck Society.

ORCID iDs

Bjoern Kscheschinski https://orcid.org/0009-0002-8226-1820
Mirna Kramar https://orcid.org/0000-0002-1637-140X
Karen Alim https://orcid.org/0000-0002-2527-5831

References

[1] Goldstein R E and van de Meent J-W 2015 A physical perspective on cytoplasmic streaming *Interface Focus* **5** 20150030
[2] Koslover E F, Chan C K and Theriot J A 2017 Cytoplasmic flow and mixing due to deformation of motile cells *Biophys. J.* **113** 2077–87
[3] Gross P, Kumar K V and Grill S W 2017 How active mechanics and regulatory biochemistry combine to form patterns in development *Annu. Rev. Biophys.* **46** 337–56
[4] Turing A M 1990 The chemical basis of morphogenesis *Bull. Math. Biol.* **52** 153–97
[5] Alim K, Amselem G, Peaudecerf F, Brenner M P and Pringle A 2013 Random network peristalsis in *Physarum polycephalum* organizes fluid flows across an individual *Proc. Natl Acad. Sci.* **110** 13306–11
[6] Alim K, Andrew N, Pringle A and Brenner M P 2017 Mechanism of signal propagation in *Physarum polycephalum Proc. Natl Acad. Sci.* **114** 5136–41
[7] Nakagaki T, Kobayashi R, Nishiura Y and Ueda T 2004 Obtaining multiple separate food sources: behavioural intelligence in the *Physarum plasmodium Proc. R. Soc.* B **271** 2305–10
[8] Nakagaki T, Yamada H and Tóth A 2000 Maze-solving by an amoeboid organism *Nature* **407** 470
[9] Tero A, Takagi S, Saigusa T, Ito K, Bebber D P, Fricker M D, Yumiki K, Kobayashi R and Nakagaki T 2010 Rules for biologically inspired adaptive network design *Science* **327** 439–42
[10] Bäuerle F K, Kramar M and Alim K 2017 Spatial mapping reveals multi-step pattern of wound healing in *Physarum polycephalum J. Phys. D: Appl. Phys.* **50** 434005
[11] Kramar M and Alim K 2021 Encoding memory in tube diameter hierarchy of living flow network *Proc. Natl Acad. Sci.* **118** e2007815118
[12] Berridge M J, Bootman M D and Roderick H L 2003 Calcium signalling: dynamics, homeostasis and remodelling *Nat. Rev. Mol. Cell Biol.* **4** 517–29
[13] Reddy A S 2001 Calcium: silver bullet in signaling *Plant Sci.* **160** 381–404
[14] Clapham D E 2007 Calcium signaling *Cell* **131** 1047–58
[15] Carafoli E and Krebs J 2016 Why calcium? How calcium became the best communicator *J. Biol. Chem.* **291** 20849–57
[16] Carafoli E 2002 Calcium signaling: a tale for all seasons *Proc. Natl Acad. Sci.* **99** 1115–22
[17] Kohama K, Kobayashi K and Mitani S 1980 Effects of Ca ion and ADP on superprecipitation of myosin B from slime mold, *Physarum polycephalum Proc. Japan Acad.* B **56** 591–6
[18] Kohama K and Kendrick-Jones J 1986 The inhibitory Ca^{2+}-regulation of the actin-activated Mg-ATPase activity of myosin from *Physarum polycephalum* plasmodia *J. Biochem.* **99** 1433–46
[19] Kohama K 2016 Calcium inhibition as an intracellular signal for actin–myosin interaction *Proc. Japan Acad.* B **92** 478–98
[20] Kessler D, Eisenlohr L, Lathwell M, Huang J, Taylor H, Godfrey S and Spady M 1980 Physarum myosin light chain binds calcium *Cell Motil.* **1** 63–71
[21] Yoshiyama S, Ishigami M, Nakamura A and Kohama K 2010 Calcium wave for cytoplasmic streaming of *Physarum polycephalum Cell Biol. Int.* **34** 35–40
[22] Zhang S, Guy R D, Lasheras J C and Del Álamo J C 2017 Self-organized mechano-chemical dynamics in amoeboid locomotion of *Physarum* fragments *J. Phys. D: Appl. Phys.* **50** 204004
[23] Julien J-D and Alim K 2018 Oscillatory fluid flow drives scaling of contraction wave with system size *Proc. Natl Acad. Sci.* **115** 10612–7
[24] Radszuweit M, Alonso S, Engel H and Bär M 2013 Intracellular mechanochemical waves in an active poroelastic model *Phys. Rev. Lett.* **110** 138102
[25] Kulawiak D A, Löber J, Bär M and Engel H 2019 Active poroelastic two-phase model for the motion of *Physarum* microplasmodia *PLoS One* **14** e0217447
[26] Daniel J W and Rusch H P 1961 The pure culture of *Physarum polycephalum* on a partially defined soluble medium *Microbiology* **25** 47–59
[27] Daniel J W, Kelley J and Rusch H P 1962 Hematin-requiring plasmodial myxomycete *J. Bacteriol.* **84** 1104–10
[28] Donahue B S and Abercrombie R 1987 Free diffusion coefficient of ionic calcium in cytoplasm *Cell Calcium* **8** 437–48
[29] Naib-Majani W, Teplov V and Baranowski Z 1988 *Morphology and Visco-Elastic Properties of Physarum Strands During the Steady-State of Their Contractile Behavior* (Springer) pp 57–63
[30] Taylor G I 1953 Dispersion of soluble matter in solvent flowing slowly through a tube *Proc. R. Soc.* A **219** 186–203
[31] Marbach S and Alim K 2019 Active control of dispersion within a channel with flow and pulsating walls *Phys. Rev. Fluids* **4** 114202
[32] Glogauer M, Arora P, Yao G, Sokholov I, Ferrier J and McCulloch C 1997 Calcium ions and tyrosine phosphorylation interact coordinately with actin to regulate cytoprotective responses to stretching *J. Cell Sci.* **110** 11–21
[33] Matthews B D, Overby D R, Mannix R and Ingber D E 2006 Cellular adaptation to mechanical stress: role of integrins, Rho, cytoskeletal tension and mechanosensitive ion channels *J. Cell Sci.* **119** 508–18
[34] Vogel V and Sheetz M 2006 Local force and geometry sensing regulate cell functions *Nat. Rev. Mol. Cell Biol.* **7** 265–75
[35] Lee J, Ishihara A, Oxford G, Johnson B and Jacobson K 1999 Regulation of cell movement is mediated by stretch-activated calcium channels *Nature* **400** 382–6
[36] Nakagaki T, Yamada H and Ueda T 1999 Modulation of cellular rhythm and photoavoidance by oscillatory irradiation in the *Physarum* plasmodium *Biophys. Chem.* **82** 23–28
[37] Yoshimoto Y, Kuroda K and Hiramoto Y 1988 Visualization of Ca^{2+} localization in caffeine-treated endoplasmic drops of *Physarum* plasmodium *Proc. Japan Acad.* B **64** 109–12